ResearchGate

See discussions, stats, and author profiles for this publication at: https://www.researchgate.net/publication/235393827

Electronegativity, Charge Transfer, Crystal Field Strength, and the Point Charge Model Revisited

ARTICLE *in* THE JOURNAL OF PHYSICAL CHEMISTRY A · JANUARY 2013

Impact Factor: 2.69 · DOI: 10.1021/jp3117566 · Source: PubMed

CITATIONS
5

READS
72

2 AUTHORS:

Peter Anthony Tanner
The Hong Kong Institute of Education
355 PUBLICATIONS **4,367** CITATIONS
SEE PROFILE

Lixin Ning
Anhui Normal University
63 PUBLICATIONS **425** CITATIONS
SEE PROFILE

Available from: Peter Anthony Tanner
Retrieved on: 26 January 2016

THE JOURNAL OF PHYSICAL CHEMISTRY A

Article

pubs.acs.org/JPCA

Electronegativity, Charge Transfer, Crystal Field Strength, and the Point Charge Model Revisited

Peter A. Tanner*,† and Lixin Ning‡

†Department of Science and Environmental Studies, The Hong Kong Institute of Education, 10 Lo Ping Street, Tai Po, Hong Kong S.A.R., P.R. China

‡Department of Physics, Anhui Normal University, Wuhu, Anhui 241000. P.R. China

Supporting Information

ABSTRACT: Although the optical spectra of $LnCl_6^{3-}$ systems are complex, only two crystal field parameters, B_{40} and B_{60}, are required to model the J-multiplet crystal field splittings in octahedral symmetry. It is found that these parameters exhibit R^{-5} and R^{-7} dependence, respectively, upon the ionic radius Ln^{3+}(VI), but not upon the Ln−Cl distance. More generally, the crystal field strengths of LnX_6 systems (X = Br, Cl, F, O) exhibit linear relationships with ligand electronegativity, charge transfer energy, and fractional ionic character of the Ln−X bond.

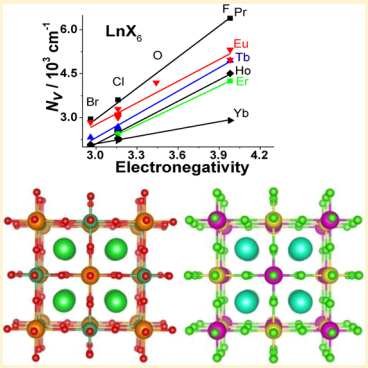

1. INTRODUCTION

Figure 1a shows the emission spectra of two europium (Eu^{3+}) ion solid-state systems: Ba_2YNbO_6 (Figure 1b, doped with Eu^{3+}) and neat $Cs_2NaEuCl_6$ (Figure 1c), which comprise EuX_6, X = O, Cl moieties, respectively. The spectra are recorded at low temperature so that features are more clearly resolved. Both spectra have previously been interpreted in detail[1−3] as arising from intraconfigurational $4f^6$ electronic and vibronic transitions from the ^5D_J (J = 0, 1) states of Eu^{3+} to the levels of the ^7F_J (J = 0−6) multiplet term (Figure 1d). The notation $^{2S+1}L_J$ concisely gives the electron spin (S), orbital (L), and total (J) angular momentum of the Eu^{3+} multiplet. The spectra are complex and a chemist might ask, "What information can we get from such spectra, and how can we condense this information?" This study throws some light upon these questions.

Knowledge of the vibrations of these systems, together with the study of the absorption spectra, enables spectral assignments to be made for the $4f^6$ energy levels. These energy levels correspond to just two multiplets: ^5D and ^7F, which are each split into $2L + 1$ states by spin−orbit coupling, and most of these states are further split by the crystal field (Figure 1d). The symmetry of these systems is octahedral for $Cs_2NaEuCl_6$, or nearly so for Ba_2YNbO_6:Eu^{3+}, and the crystal field may be modeled by two crystal field parameters (CFP), B_{kq}, namely, B_{40} and B_{60}, as has previously been performed.[3,4] These two parameters summarize concisely the crystal field splittings of multiplets. An attempt was made to provide a physical meaning for the crystal field parameters in a previous publication.[4] In the present study, the relationships between crystal field parameters, crystal field strength, electronegativity and fractional ionic character are investigated.

2. THEORY

The simplest theoretical model, the point charge electrostatic model (PCEM)[5,6] envisages the electrostatic field experienced by the lanthanide ion to result from the external charge densities in the crystal, modeled as point charges. The expressions for the parameters for the case of octahedral symmetry of Ln^{3+} are particularly simple:[5]

$$B_{40} = (-7/2)Z_{eff}e^2\langle r^4\rangle R^{-5} \quad (1)$$

$$B_{60} = (-3/4)Z_{eff}e^2\langle r^6\rangle R^{-7} \quad (2)$$

where r is the 4f radial coordinate, and $\langle r^k\rangle$ denotes the mean value of r^k relative to the $R_{4f}(r)$ function, R is the metal−ligand distance, and $Z_{eff}e$ is the effective ligand charge.

The ratio of B_{40}/B_{60} according to the PCEM is

$$\text{Ratio}(B_{40}/B_{60}) = (14/3)[\langle r^4\rangle/\langle r^6\rangle]R^2 \quad (3)$$

The expression for the scalar crystal field strength is

$$N_v = \left[\sum_{k,q}\frac{4\pi}{2k+1}(B_{kq})^2\right]^{1/2} \quad (4)$$

For LnX_6^{3-}, with O_h site symmetry of Ln^{3+}, only k = 4, 6 and q = 0, ±4 are nonzero, and

Received: November 29, 2012
Revised: January 29, 2013
Published: January 30, 2013

ACS Publications © 2013 American Chemical Society

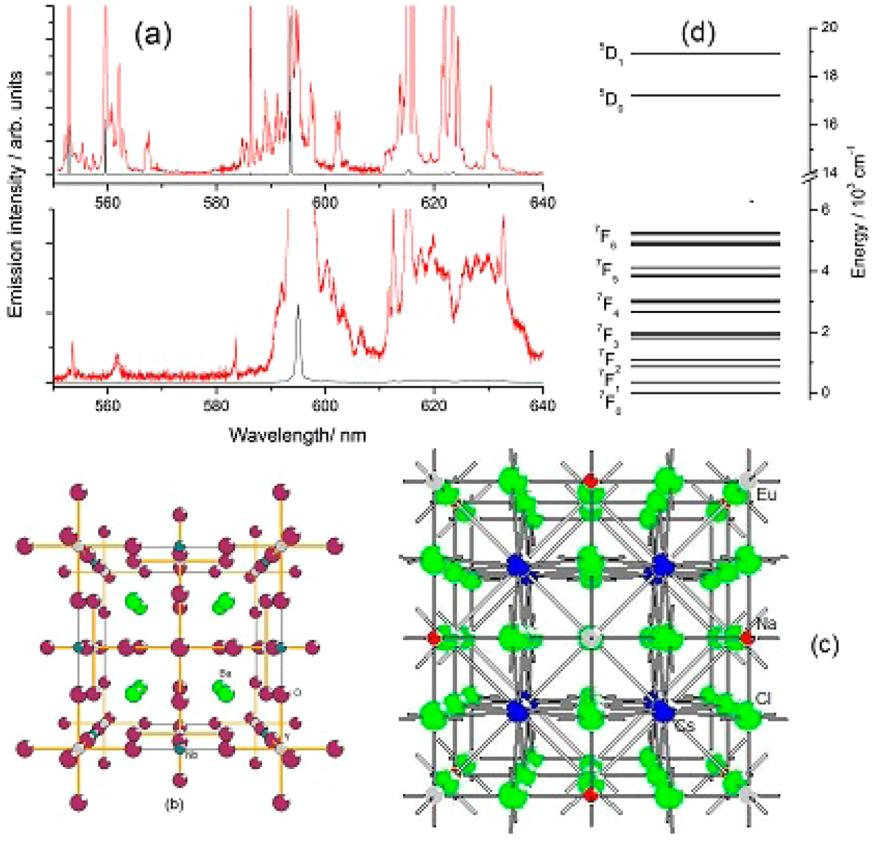

Figure 1. (a) 10 K emission spectra of $Cs_2NaEuCl_6$ (top: 465 nm excitation) and Ba_2YNbO_6:Eu^{3+} (bottom: 528.5 nm excitation) between 550 and 640 nm, with scale expansions of 100 times in red. The most intense band at 593−594 nm corresponds to the $^5D_0 \rightarrow {}^7F_1$ transition. (b), (c) Crystal structures of Ba_2YNbO_6 and $Cs_2NaEuCl_6$. (d) Lower energy level scheme of Eu^{3+}.

$$B_{4\pm4} = \sqrt{\frac{5}{14}}\,B_{40} \text{ and } B_{6\pm4} = -\sqrt{\frac{7}{2}}\,B_{60} \tag{5}$$

Besides, because $B_{40} \gg B_{60}$ for LnX_6^{3-},[4] the sixth-rank B_{kq} can be omitted. Then,

$$\begin{aligned} N_v &= \left[\sum_{k,q} \frac{4\pi}{2k+1}(B_{kq})^2\right]^{1/2} \\ &= \sqrt{\frac{4\pi}{9}}\left[(B_{40})^2 + (B_{44})^2 + (B_{4-4})^2\right]^{1/2} \\ &= \frac{4}{3}\sqrt{\frac{3\pi}{7}}\,B_{40} \end{aligned} \tag{6}$$

Hence, the plot of N_v vs B_{40} is expected to have the slope 1.55. The validity of this relationship is demonstrated from experimental values of B_{40} and B_{60} from the $LnCl_6^{3-}$ series[4] in Figure S1, Supporting Information, where the slope is 1.62 ± 0.02. Because, with the PCEM model for the crystal-field interaction, the B_{40} parameter may be expressed as in eq 1, when substituting eq 6 into eq 1, we obtain

$$N_v = \sqrt{\frac{28\pi}{3}}\,(-Z_{\text{eff}}e^2)\frac{\langle r^4\rangle}{R^5} \tag{7}$$

In eq 6, the effective ligand charge Z_{eff} may be expressed as

$$Z_{\text{eff}} = f \cdot Z \tag{8}$$

where Z is the formal ionic charge of the ligands and f is the fractional ionic character of the chemical bonds. To estimate the value of f, Pauling's empirical formula may be employed:

$$f = 1 - \exp[-0.25(\chi_{\text{ln}} - \chi_X)^2] \tag{9}$$

where χ_{Ln} and χ_X are the electronegativities of the lanthanide and the ligand, respectively. Substituting eqs 8 and 9 into eq 7, we have

$$N_v = \sqrt{\frac{28\pi}{3}}\,[1 - e^{-0.25(\chi_{\text{Ln}} - \chi_L)^2}](-Ze^2)\frac{\langle r^4\rangle}{R^5} \tag{10}$$

If we repace the Ln−X distance R by the Shannon ionic radius r_{rad}, $r[Ln^{3+}(VI)]$, according to the following discussions in the text, the above expression turns into

$$N_v = \sqrt{\frac{28\pi}{3}}\,[1 - e^{-0.25(\chi_{\text{Ln}} - \chi_L)^2}](-Ze^2)\frac{\langle r^4\rangle}{r_{\text{rad}}{}^5} \tag{11}$$

3. RESULTS AND DISCUSSION

Using the Ln−Cl distances, R, from the lattice parameters of $Cs_2NaLnCl_6$ systems[7] and the values of $\langle r^k\rangle$ and B_{kq} in the Supporting Information, Figure 2a uncovers that the slope for the plot of $\log[B_{40}/\langle r^4\rangle]$ versus $\log R$ (i.e., representing the power of R), is −33.5 ± 1.8. Alternatively, using values of R from ab initio calculations,[8] the slope is −(15.8 ± 1.2). Both values would appear to show that the formula from the PCEM model is invalid. However, when the Ln^{3+}(VI) ionic radius is employed, instead of R, as in Figure 2b, the slope of −5.5 ± 0.4 is found, in reasonable agreement with eq 1. The analogous plots for B_{60} employing

dx.doi.org/10.1021/jp3117566 | J. Phys. Chem. A 2013, 117, 1503−1507

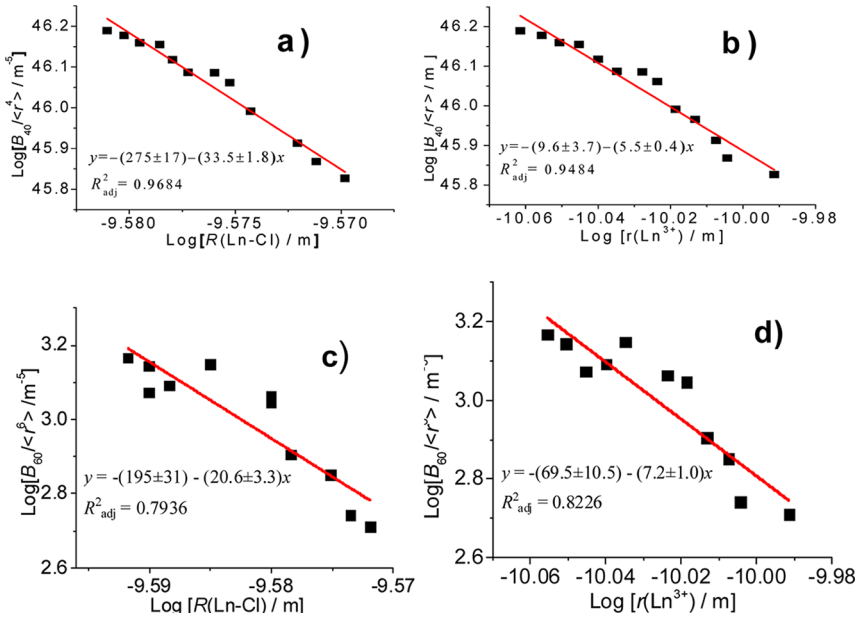

Figure 2. (a), (b) Plot of $\log[B_{40}/\langle r^6\rangle]$ and (c), (d) $\log[B_{60}/\langle r^6\rangle]$ against $\log[R(\mathrm{Ln-Cl})]$ from lattice parameter data (a), (c) and against $\log[r(\mathrm{Ln}^{3+}(\mathrm{VI})]$ from Shannon ionic radii (b), (d).

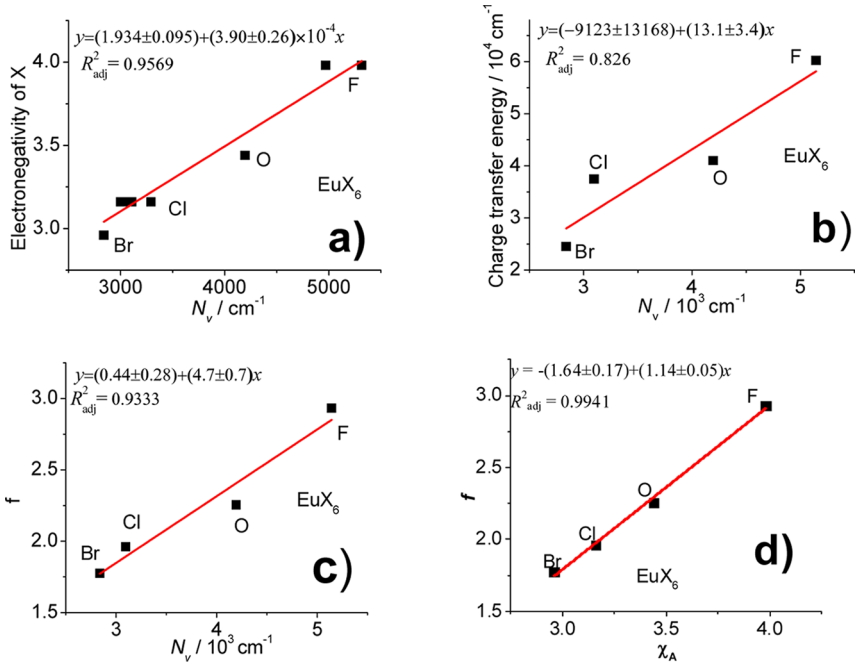

Figure 3. Plots of crystal field strength, N_v (abscissa) against (a) electronegativity, (b) charge transfer band maximum, and (c) fractional ionic character, for EuX_6 systems. (d) shows fractional ionic character vs electronegativity of X in EuX_6. Refer to the text for explanations. The N_v values in (a) are calculated from the crystal field parameters in refs 4 and 12 ($Cs_2NaEuCl_6$ and Cs_2NaYCl_6: Eu^{3+}); refs 13 and 14 (Cs_2NaYF_6:Eu^{3+}); ref 3 (Ba_2YNbO_6:Eu^{3+}); and the fitting of the energy level data in ref 15 ($Cs_2NaLuBr_6$: Eu^{3+}). In Figure 2b, the CT maxima are taken from the values given in ref 16 ($Cs_2NaEuCl_6$), ref 17 (Cs_2NaYF_6:Eu^{3+}), refs 16, 18, and 19 (Y_2O_3:Eu^{3+} and EuO_6^{9-} impurities), and ref 20 ($EuBr_6^{3-}$ in tetraethylammonium bromide saturated anhydrous acetonitrile solution).

R(Ln−Cl) from the lattice parameter and $r(\mathrm{Ln}^{3+}(\mathrm{VI}))$ yield slopes of $-(20.6 \pm 3.3$ and -7.2 ± 1.0, respectively (Figure 2c,d), compared with the value 7.0 from eq 2. These results are taken to mean that the Ln^{3+}–ligand interaction is ionic and that the point charges are not located at the distance R(Ln−Cl) but at the distance $r(\mathrm{Ln}^{3+})$.

The values of the Ratio(B_{40}/B_{60}) (eq 3) for Pr^{3+} and Tm^{3+} in $Cs_2NaLnCl_6$ are, respectively, 8.6 and 9.8 from the experimental data fitting given in ref 4, 3.0 and 3.4 by using ionic radii $r[\mathrm{Ln}^{3+}(\mathrm{VI})]$ in eq 3, and 22.3 and 30.7 by using R(Ln−Cl) from the lattice parameters in eq 3. The agreement is better when ionic radii are used instead of ligand–metal distances.

Although this modified PCEM model underestimates the ratio of B_{40}/B_{60}, it provides a reasonable guide to the power variations of crystal field parameters with distance so that we now pursue it further. Note that the slower variation (r^{-5}) of B_{40} with distance leads to its dominance over B_{60} for the $LnCl_6^{3-}$ elpasolite systems, and it is also responsible for the dominance of the Cl^- nearest neighbor contribution to the crystal field.

dx.doi.org/10.1021/jp3117566 | J. Phys. Chem. A 2013, 117, 1503−1507

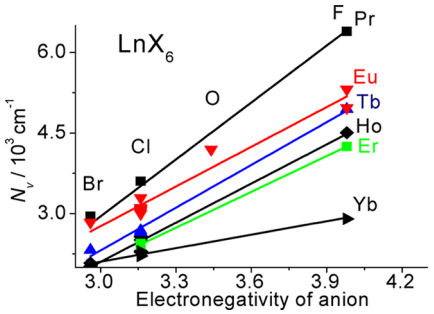

Figure 4. Plot of N_v against electronegativity of anion for LnX_6 moieties. Data from refs 3, 4, 12, 14, 15, and 22−28.

The crystal field data can be summarized more succinctly, through the combination of the crystal field parameters to give the scalar crystal field strength, N_v, defined in eq 4.[9,10] This strength, which is an invariant (i.e., it does not change under a transformation from one coordinate system to another) is related to the maximum splitting of a given J state of a rare earth ion in a crystal. It is a quantity that can characterize the crystal field strength in any kind of symmetry. To a chemist, interactions between ions lie in the realm of bonding, and ionic bonds concern those between atoms of widely different electronegativity. Sen has stated that electronegativity not only is an intuitive concept but also can be treated as a quantum chemical parameter.[11] The crystal field strengths derived for EuX_6 systems (X = Br, Cl, F, O) are plotted against the corresponding Pauling electronegativities of X, χ_X, in Figure 3a and a linear relation is found. The scatter in the values of crystal field strength for an individual EuX_6 system shows the typical errors in determination of N_v. These errors mainly arise from (i) different numbers of parameters employed in the energy level fitting, (ii) different numbers of energy levels employed in the fits, (iii) incorrect spectral assignments, and (iv) errors in the calculation. The most electronegative ligand, F, representing the closest ligand and most ionic bonding, exhibits the largest value of N_v, in LnF_6^{3-}.

Jørgensen gave a relationship between optical electronegativity and the position of the charge transfer (CT) band of a lanthanide ion system.[21] In fact, the optical electronegativities are directly proportional to electronegativity values, so that a correlation is then expected between the CT band maximum and N_v. Estimations of CT band maxima for Eu^{3+} are taken from the available literature and it is noted that the band positions are approximate because they vary according to the synthesis method and history of the sample, as well exhibiting marked differences in solution compared with the solid state. For example, the CT band of Eu−O in six coordination in the solid state is estimated to be between 39200 and 43103 cm^{-1}.[1,16,19,22] Thus, Figure 3b shows the approximate linear relationship between CT band energy and N_v for the EuX_6 systems. The CT energy relates to the two-center process in a crystal:

$$Ln^{3+}\,(GS) + VB \rightarrow Ln^{2+}\,(GS\text{: vibrationally excited}) + VB\,(hole) \quad (12)$$

where GS refers to ground electronic state, and the valence band (VB) is mainly composed of ligand p-electrons. The electron transfer is easier if the Ln−X bond is weak, i.e., small N_v. From the linear relations in Figure 2a,b, an estimation of N_v for the EuI_6^{3-} complex is 1640 ± 190 cm^{-1}, taking the Pauling electronegativity of I as 2.5 and the CT band wavelength as 675 nm.[23] This value would enable a simulation of crystal field splittings to be made for EuI_6^{3-}. Figure 3c shows that the relationship between N_v and fractional ionic character, f, of the bond (eq 9) is linear, because that between f and electronegativity is also linear for Eu−X (Figure 3d).

The linearity of the plot of N_v and electronegativity is general for LnX_6 moieties (Figure 4). The ordinate intercept of the plot becomes less negative (Figure S1a, Supporting Information), and the slope becomes less positive (Figure S1b, Supporting Information), as the number of electrons in $4f^N$ increases. This indicates a smaller discrimination in N_v values for the different ligands when the lanthanide cation is smaller and more polarizing, which is a consequence of the smaller N_v values for the smaller cations, as shown for the $LnCl_6^{3-}$ series in Figure 5a. The corresponding relation is also found for LnO_6 systems (Figure 5b) but the N_v values were calculated from very incomplete data sets and are not as accurate. A similar linear plot has previously been given for B_{40} and the number of 4f-electrons.[4] The relations involving N_v (Figures 5a,b) ensue because B_{40} dominates over B_{60} for the LnX_6 systems so that it is linearly proportional to N_v (Figure S1, Supporting Information, and eq 6). This dominance of B_{40} results from its distance dependence, the predominantly ionic character and relatively long bond distances in LnX_6 systems. This dominance of B_{40}, and the presence of such simple linear relations as presented herein, are unlikely to exist generally for other Ln^{3+} systems where more than two crystal field parameters are involved, or even for the T_h symmetry systems $Ln(NO_2)_6^{3-}$.[29]

4. CONCLUSIONS

In summary, the small number of crystal field parameters for the O_h symmetry systems LnX_6 has enabled a simple rationalization of the different concepts: crystal field strength, electronegativity, and charge transfer. The point charge electrostatic model has been shown to provide an approximate basis for these

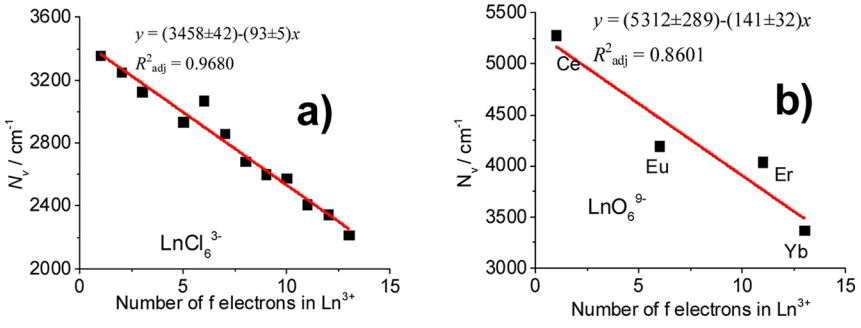

Figure 5. Plot of N_v against number of 4f electrons of Ln^{3+} in (a) $LnCl_6^{3-}$ (data from ref 4) and (b) LnO_6^{9-} (data from refs 3, 31, and 30. In ref 30, the multiplicative factors arising from the reduced matrix elements were omitted from the values of crystal field parameters.).

dx.doi.org/10.1021/jp3117566 | J. Phys. Chem. A 2013, 117, 1503−1507

relationships. It has been demonstrated that the PCEM model, which has previously been thought to give only the correct signs of the crystal field parameters, can be used to rationalize the distance dependence of the crystal field strengths, (or crystal field parameters) of the elpasolite and double perovskite systems. This rationalization using the ionic radius of Ln^{3+}(VI) points to (or confirms) the important fact that the localization of Ln^{3+} 4f electrons remains in an inorganic compound with negligible contribution to bonding.

■ ASSOCIATED CONTENT

Supporting Information

Plot of N_v against fourth rank crystal field parameter for $LnCl_6^{3-}$ systems (Figure S1); plots of (a) intercept and (b) slope from Figure 4 (Figure S2); and table of crystal field parameters and radial integrals. This material is available free of charge via the Internet at http://pubs.acs.org.

■ AUTHOR INFORMATION

Corresponding Author

*E-mail: peter.a.tanner@gmail.com.

Notes

The authors declare no competing financial interest.

■ ACKNOWLEDGMENTS

L.N. acknowledges support from the National Natural Science Foundation of China (Grant No. 11174005).

■ REFERENCES

(1) Morley, J. P.; Faulkner, T. R.; Richardson, F. S. *J. Chem. Phys.* **1982**, *77*, 1710−1723.
(2) Thorne, J. R. G.; Jones, M.; McCaw, C. S.; Murdoch, K. M.; Denning, R. G.; Khaidukov, N. M. *J. Phys.: Condens. Matter* **1999**, *11*, 7851−7866.
(3) Li, W.; Ning, L.; Tanner, P. A. *J. Phys. Chem. A* **2012**, *116*, 7337−7344.
(4) Duan, C.-K.; Tanner, P. A. *J. Phys. Chem. A* **2010**, *114*, 6055−6062.
(5) Görller-Walrand, C.; Binnemans, K. In *Handbook on the Physics and Chemistry of Rare Earths*; Gschneidner, K. A., Jr., Eyring, L., Eds.; Elsevier Science B.V.: Amsterdam, 1996; Vol. *23*, Chapter 155, pp 121−283.
(6) Garcia, D.; Faucher, M. In *Handbook on the Physics and Chemistry of Rare Earths*; Gschneidner, K. A., Jr., Eyring, L., Eds.; Elsevier Science B.V.: Amsterdam, 1995; Vol. *21*, Chapter 144, pp 263−304.
(7) Meyer, G. *Prog. Solid. State Chem.* **1982**, *14*, 141−219.
(8) Ordejon, B.; Seijo, L.; Barandiaran, Z. *J. Chem. Phys.* **2003**, *119*, 6143−6149.
(9) Auzel, F. *Opt. Mater.* **2002**, *19*, 89−94.
(10) Auzel, F.; Malta, O. *J. Phys. (Paris)* **1983**, *44*, 201−206.
(11) Sen, K. D. In *Structure and Bonding (Berlin)*; Sen, K. D.; Jørgensen, C. K., Eds.; Springer-Verlag: Berlin, 1987; Vol. *36*, front page No. 4.
(12) Tanner, P. A.; Ravi Kanth Kumar, V. V.; Jayasankar, C. K.; Reid, M. F. *J. Alloys Compd.* **1994**, *215*, 349−370.
(13) Thorne, J. R. G.; Jones, M.; McCaw, C. S.; Murdoch, K. M.; Denning, R. G.; Khaidukov, N. M. *J. Phys.: Condens. Matter* **1999**, *11*, 7851−7866.
(14) Tanner, P. A.; Liu, Y.-L.; Edelstein, N.; Murdoch, K.; Khaidukov, N. M. *J. Phys.: Condens. Matter* **1997**, *9*, 7817−7836.
(15) Dushin, R. B.; Barbanel, Y. A.; Kolin, V. V.; Kotlin, V. P.; Nekhoroshkov, S. N.; Chudnovskaya, G. P. *Radiochemistry* **2000**, *42*, 53−60.
(16) Duan, C.-K.; Tanner, P. A.; Meijerink, A.; Babin, V. *J. Phys.: Condens. Matter* **2009**, *21*, 395501 (9 pp.)..
(17) Tanner, P. A.; Duan, C.-K.; Makhov, V. N.; Kirm, M.; Khaidukov, N. M. *J. Phys.: Condens. Matter* **2009**, *21*, 395504 (10 pp).
(18) Dorenbos, P. *J. Phys.: Condens. Matter* **2003**, *15*, 8417−8434.
(19) Tanner, P. A.; Fu, L.; Cheng, B.-M. *J. Phys. Chem. C* **2009**, *113*, 10773−10779.
(20) Nugent, L. J.; Baybarz, R. D.; Burnett, J. L.; Ryan, J. L. *J. Phys. Chem.* **1973**, *77*, 1528−1539.
(21) Jørgensen, C. K. *Mol. Phys.* **1963**, *6*, 43−47.
(22) Duan, C.-K.; Tanner, P. A.; Babin, V.; Meijerink, A. *J. Phys. Chem. C* **2009**, *113*, 12580−12585.
(23) Ryan, J. L. *Inorg. Chem.* **1969**, *8*, 2053−2058.
(24) Zhou, X.; Reid, M. F.; Faucher, M. D.; Tanner, P. A. *J. Phys. Chem. B* **2006**, *110*, 14939−14942.
(25) Zhou, X.; Tanner, P. A.; Faucher, M. D. *J. Phys. Chem. C* **2007**, *111*, 683−687.
(26) Tanner, P. A.; Faucher, M. D.; Zhou, X. *J. Phys. Chem. A* **2011**, *115*, 2557−2567.
(27) McCaw, C. S.; Murdoch, K. M.; Denning, R. G. *Mol. Phys.* **2003**, *101*, 427−438.
(28) Berry, A. J.; Morrison, I. D.; Denning, R. G. *Mol. Phys.* **1998**, *93*, 1−14.
(29) Tanner, P. A.; Li, W.; Ning, L. *Inorg. Chem.* **2012**, *51*, 2997−3006.
(30) Calder, S.; Fennell, T.; Kockelmann, W.; Lau, G. C.; Cava, R. J.; Bramwell, S. T. *J. Phys.: Condens. Matter* **2010**, *22*, 116007 (7 pp.)..
(31) Zhou, W.-L.; Zhang, Q.-L.; Gao, J.-Y.; Liu, W.-P.; Ding, L.-H.; Yin, S.-T. *Chin. Phys. B* **2011**, *20*, 016101 (8 pp).